Different modes of SecY–SecA interactions revealed by site-directed *in vivo* photo-cross-linking

Hiroyuki Mori and Koreaki Ito*

Institute for Virus Research, Kyoto University, Kyoto 606-8507, Japan

Edited by Tom A. Rapoport, Harvard Medical School, Boston, MA, and approved September 7, 2006 (received for review July 27, 2006)

While the SecA ATPase drives protein translocation across the bacterial cytoplasmic membrane by interacting with the SecYEG translocon, molecular details of SecA–SecY interaction remain poorly understood. Here, we studied SecY–SecA interaction by using an *in vivo* site-directed cross-linking technique developed by Schultz and coworkers [Chin, J. W., Martin, A. B., King, D. S., Wang, L., Schultz, P. G. (2002) *Proc. Natl. Acad. Sci. USA* 99:11020–11024 and Chin, J. W., Schultz, P. G. (2002) *ChemBioChem* 3:1135–1137]. Benzoyl-phenylalanine introduced into specific SecY positions at the second, fourth, fifth, and sixth cytoplasmic domains allowed UV cross-linking with SecA. Cross-linked products exhibited two distinct electrophoretic mobilities. SecA cross-linking at the most C-terminal cytoplasmic region (C6) was specifically enhanced in the presence of NaN_3, which arrests the ATPase cycle, and this enhancement was canceled by cis placement of some *secY* mutations that affect SecY–SecA cooperation. *In vitro* experiments showed directly that SecA approaches C6 when it is engaging in ATP-dependent preprotein translocation. On the basis of these findings, we propose that the C6 tail of SecY interacts with the working form of SecA, whereas C4–C5 loops may offer constitutive SecA-binding sites.

protein translocation | translocon

Sec-mediated protein translocation takes place via the evolutionarily conserved translocon, SecYEG in prokaryotes and Sec61$\alpha\beta\gamma$ in eukaryotes (1). These channel-like transmembrane complexes (2) can cooperate with different cytosolic components. In bacteria, SecYEG participates in both the SRP- and ribosome-dependent cotranslational integration of membrane proteins and the SecB- and SecA-dependent posttranslational translocation of periplasmic and outer membrane proteins (3, 4). The crucial factor for the latter process is the SecA ATPase that drives preprotein movement into and across the translocon (5). In doing so, a SecA–preprotein complex must interact specifically with SecYEG (6), leading to its large conformational changes coupled with the ATP hydrolysis cycles (7).

SecY has 10 transmembrane regions (TM1–TM10, numbered from amino to carboxyl termini), six cytoplasmic regions (C1–C6), and five periplasmic regions (P1–P5) (ref. 8; see also Fig. 1*A*), with its N-terminal (TM1–TM5) and C-terminal (TM6–TM10) halves arranged pseudosymmetrically in three dimensions (2). It forms a heterotrimeric complex, having an hourglass-shaped narrow pathway for polypeptide transit in the SecY portion. Although a single unit of the trimer is thought to serve as a translocation channel (2, 9), exact oligomeric state of the heterotrimer has not been established (10–14).

SecA binds with high affinity to membranes containing SecYEG (15), which stimulates the SecA ATPase activity (16). Although cross-linking experiments using formaldehyde treatment of the cell detected direct cross-linked products between SecA and SecY (17), SecA-binding sites on the SecY molecule have not been identified. SecA-binding assays using truncated SecY polypeptides fixed onto membrane filters suggested that a N-terminal region of SecY binds SecA (18). However, it is difficult to evaluate the significance of the results obtained in such artificial experimental settings. In the structure of the translocon, the C-terminal half of SecY contains relatively large C4–C6 protrusions, which were postulated to act as a platform for binding of cytosolic factors, such as the ribosome and SecA (2).

Although site-directed chemical cross-linking approaches are effective for studying arrangements of subunits, such as SecY–SecG and SecY–SecE, of the constitutively formed SecYEG complex (19–21), they may not be effective enough to reveal transient association of SecYEG with SecA that should undergo dynamic conformational changes during the functioning. Our genetic and biochemical studies revealed that the C5 and C6 regions of SecY are indeed important for supporting the translocase function of SecA (6, 22–25). Whereas mutations such as *secY39* (Arg-357–His in C5) (24, 26) and *secY205* (Tyr-429–Asp in C6) compromise the functioning of SecA, including its "insertion" ability, compensatory or up-regulating alterations in SecA suppress such defects (6, 27). Other mutations in *secY*, known as *prl* (28) and "super active" (29) alleles, apparently allow more effective utilization of SecA.

In this work, we attempted to study *in vivo* interaction between SecY and SecA, using the innovative technique developed by Schultz and colleagues (30, 31) that allows site-directed *in vivo* cross-linking. In this experimental system, an *amber* suppressor tRNA and a tyrosyl-tRNA synthetase from *Methanococcus jannaschii* are mutated to allow the charging of the tRNA with *p*-benzoyl-phenylalanine (pBPA), a photo-reactive phenylalanine derivative (32). The benzophenone group of pBPA reacts with a nearby C-H bond upon excitation at 350–365 nm, and its positioning in the primary target protein can be manipulated by introduction of an *amber* (TAG) codon. Thus, we carried out *in vivo* cross-linking using SecY mutants having *amber* codons in the cytosolic regions. UV irradiation of cells cultivated in the presence of pBPA revealed marked cross-linking with SecA at specific SecY positions. We thus identified SecY residues that are adjacent to SecA *in vivo*. Among them, residues at C6 were found to be approached by a working form of SecA as it is driving preprotein translocation.

Results

The Feasibility of Using Site-Directed *in Vivo* Cross-Linking with SecY. We tested the technique of Chin *et al.* (30) at three positions of SecY previously shown to be near neighbors of SecG or SecE (19, 20). We introduced two plasmids into *Escherichia coli* cells, one encoding the *amber* suppressor tRNA and the engineered tyrosyl-tRNA synthetase (30) and the other encoding a SecY–His_6–Myc with an *amber* mutation at positions 117, 179, or 354. As presented in *Supporting Text*, which is published as supporting

Author contributions: H.M. and K.I. designed research; H.M. performed research; H.M. and K.I. analyzed data; and H.M. and K.I. wrote the paper.

The authors declare no conflict of interest.

This article is a PNAS direct submission.

Freely available online through the PNAS open access option.

Abbreviations: pBPA, *p*-benzoyl-phenylalanine; IMV, inverted membrane vesicle.

*To whom correspondence should be addressed. E-mail: kito@virus.kyoto-u.ac.jp.

© 2006 by The National Academy of Sciences of the USA

BIOCHEMISTRY

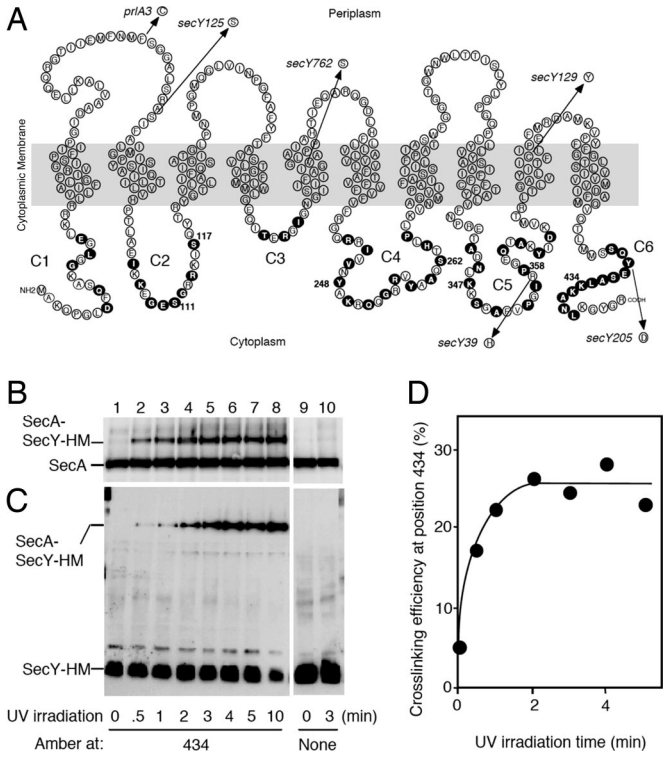

Fig. 1. Target SecY residues and SecY–SecA cross-linking conditions. (*A*) The amino acid residues of SecY are displayed to indicate cytoplasmic (C1–C6), transmembrane, and periplasmic regions (8). The residues individually mutated to *amber* in this study are indicated by solid circles. The SecY alterations that were introduced additionally into some of the *amber* mutants are shown by arrows with allele names. (*B–D*) Demonstration of *in vivo* photo-cross-linking between SecY and SecA. Cells expressing the *amber* 434 mutant of SecY–His_6–Myc (lanes 1–8) or WT SecY–His_6–Myc (lanes 9 and 10) were grown in the presence of pBPA, treated with 0.08% NaN_3 for 5 min, and UV-irradiated for the indicated periods of time (min). Membrane proteins were separated by 7.5% SDS/PAGE and analyzed by anti-SecA (*B*) and anti-Myc (*C*) immunoblotting. The cross-linked proportions (%) in the membrane-associated SecA molecules (*B*) are depicted graphically in *D*.

information on the PNAS web site, *amber* fragments of SecY were detected in the absence of pBPA, whereas growth in the presence of pBPA led to the production of the full-size SecY-His_6-Myc (Fig. 7, which is published as supporting information on the PNAS web site). The SecYEG–His_6–Myc (*amber*) plasmids were also shown to pBPA-dependently complement the growth defect caused by the chromosomal *secY39*(Cs) mutation (data not shown). Thus, introduction of pBPA, at least into the positions examined above, does not interfere with the functioning of SecY. UV irradiation of the pBPA-grown cells led to the formation of a SecY–SecG or a SecY–SecE cross-linked product as expected (Fig. 7). Thus, the *in vivo* cross-linking approach can effectively address the subunit interactions of the SecYEG complex.

Cross-Linking Between SecY and SecA. To survey cytosolic residues of SecY for their proximity to other proteins, we constructed a total of 53 *amber* mutants of SecY–His_6–Myc, as shown in Fig. 1*A*. UV irradiation of cells grown in the presence of pBPA, isolation of membranes, and their electrophoretic/immunoblotting analysis allowed us to identify a number of SecY positions at which it was cross-linkable with SecA (Fig. 2). For instance, UV irradiation of cells expressing SecY–His_6–Myc *amber–434* yielded a band above normal SecA and reacting with both anti-SecA (Fig. 1*B*) and anti-Myc (Fig. 1*C*). The appearance of this SecY–SecA cross-linked product was irradiation-dependent, reaching the maximum (≈25% conversion of the membrane-associated SecA molecules) in ≈3 min under the experimental conditions used (Fig. 1*D*). This irradiation time was used in all of the photo-cross-linking experiments in this study.

All 53 *amber* constructs were tested for *in vivo* photo-cross-linking. Immunoblotting with anti-SecA (Fig. 2) showed that the following SecY positions yielded a significant cross-linking with SecA: positions 109 and 111 in C2 (Fig. 2*B*); positions 248, 262, and 264 in C4 (Fig. 2*D*); positions 347 and 358 in C5 (Fig. 2*E*); and positions 433, 434, 435, 436, 437, and 438 in C6 (Fig. 2*F*). Interestingly, two distinct electrophoretic mobilities were noted. The products mediated by the C2 or the C5 residues migrated slower than those mediated by the residues in C4 or C6.

NaN_3 Enhances SecY Cross-Linking with SecA at C6. To correlate the degree of cross-linking to specific functional state of SecY/SecA, we carried out the photo-cross-linking both with and without prior treatment of cells with NaN_3, which is known to arrest the ATPase cycle of SecA (33) and to stabilize the "membrane-inserted" state of SecA by retarding the "de-insertion" step (34). In fact, the results presented in Fig. 2 had been obtained after NaN_3 treatment. All of the positions were tested for the effect

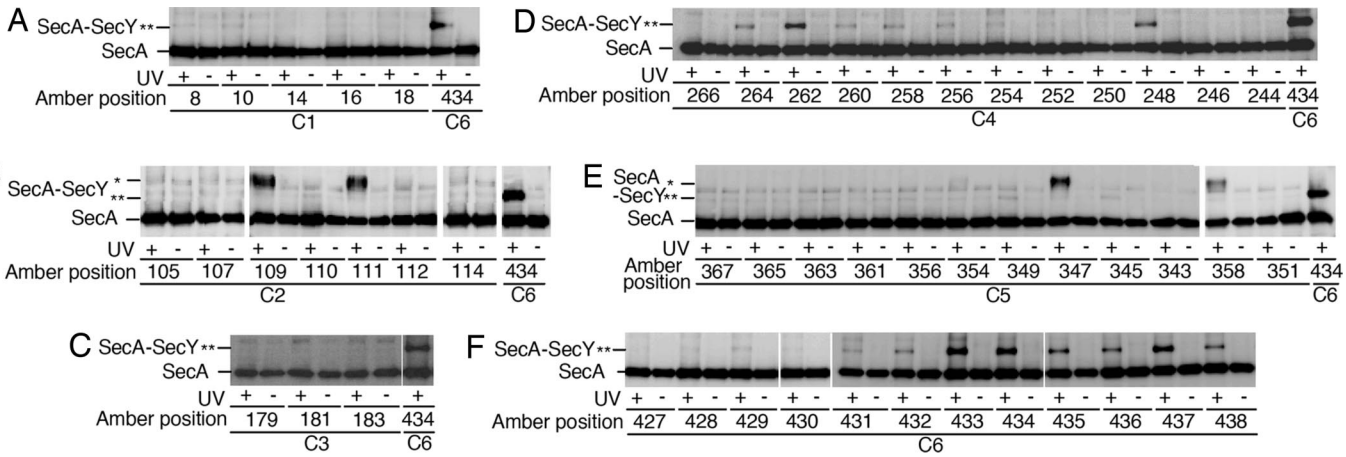

Fig. 2. Survey of the SecY cytoplasmic residues for pBPA-mediated cross-linking with SecA. Cells expressing SecY–His_6–Myc derivatives having pBPA at the indicated *amber* positions were treated with 0.08% NaN_3 for 5 min and UV-irradiated for 3 min, as indicated. Membrane fractions were analyzed by 7.5% SDS/PAGE and anti-SecA immunoblotting. Cross-liked products are indicated by * for lower mobility product and ** for higher mobility product.

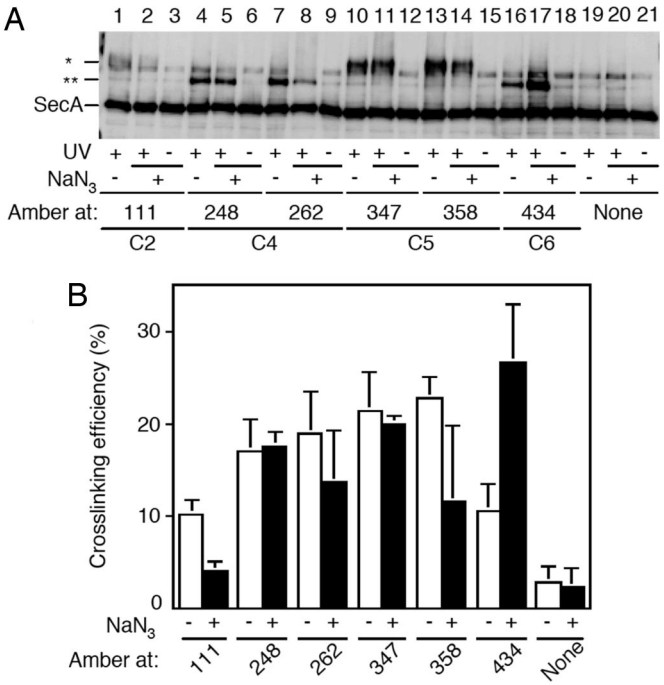

Fig. 3. Effects of NaN_3 on SecY–SecA cross-linking at different SecY positions. (*A*) Cells expressing SecY–His_6–Myc derivatives having pBPA incorporated at the indicated positions were treated with 0.08% NaN_3 for 5 min at 37°C when indicated by (NaN_3, +) and then UV-irradiated as indicated by (UV, +). Membrane fractions were analyzed by anti-SecA immunoblotting. (*B*) Averaged cross-linking efficiencies (cross-linked proportions in the membrane-bound SecA, after subtraction of nonirradiated control values) from three independent experiments are shown with error bars. Open columns, without NaN_3 treatment; solid columns, after NaN_3 treatment.

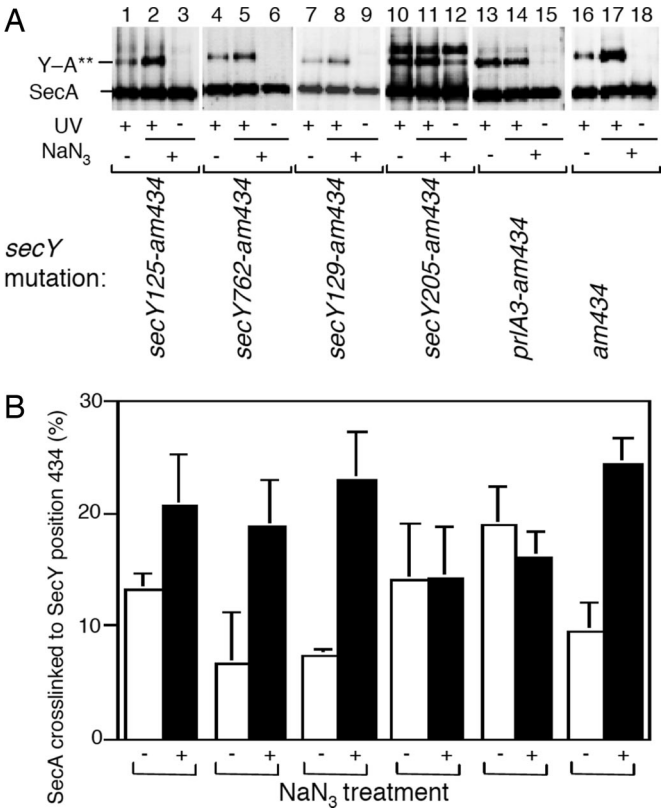

Fig. 4. Effects of function-related *secY* alterations on the SecY–SecA cross-linking at position 434. (*A*) The indicated *secY* mutations were introduced into SecY–His_6–Myc having the *amber* 434 cross-linking target. Cells expressing the resulting double mutant forms of SecY–His_6–Myc were grown in the presence of pBPA and treated with NaN_3 as indicated, followed by UV irradiation as indicated. Membranes were analyzed by anti-SecA immunoblotting. (*B*) Averaged cross-linking efficiencies (cross-linked proportions in the membrane-bound SecA, after subtraction of nonirradiated control values) from three independent experiments are shown with error bars. Open columns, without NaN_3 treatment; solid columns, after NaN_3 treatment.

of NaN_3 on cross-linking. At most positions no difference was seen. However, enhancement of cross-linking by ≈2.5 fold was seen at three positions in C6: 434 (Fig. 3*A*, lanes 16 and 17) and 433 and 437 (data not shown). A decrease in cross-linking was observed at positions 111 in C2 and 358 in C5 (Fig. 3). The C6-specific cross-linking enhancement by NaN_3 suggests that the spatial arrangement of SecA with this region of SecY undergoes significant changes during the reaction cycle of SecA.

Effects of Cis Placement of *secY* Alterations on Site-Specific *in Vivo* Cross-Linking with SecA. We addressed the functional significance of the cross-linkings further by combining selected *amber* mutants of SecY–His_6–Myc (positions 111, 248, 262, 347, 358, and 434) with the following *secY* missense alterations: *prlA3* (Phe-67–Cys) (35); *secY125* (Ser-76–Phe) (36, 37); *secY762* (Ile-195–Ser) (29); *secY39* (Arg-357–His) (24, 26); *secY129* (Cys-385–Tyr) (36); and *secY205* (Tyr-429–Asp) (6, 36). Thus, a total of 36 double mutants were constructed (strain carrying the *amber*–434–*secY39* double mutant plasmid did not grow in the presence of pBPA). They were subjected to *in vivo* cross-linking in the presence and the absence of NaN_3 (Fig. 4*A*; only data for position 434 are presented). The overall pictures of cross-linking were similar between the single and the double mutants, except that the NaN_3 response of cross-linking at position 434 in C6 was abolished by two *secY* mutations, *prlA3* and the *secY205* (Fig. 4*A*, lanes 11 and 14). The results that the NaN_3 effect is cancelled by mutational alterations affecting the SecY function are consistent with the notion that the C6–SecA distance is modulated by the SecA states of engagement in translocation.

***In Vitro* Cross-Linking at Position 434 Is Enhanced Under the Translocation Conditions.** To address the relationships between the C6–SecA cross-linking and ongoing protein translocation reaction more directly, we carried out *in vitro* experiments using inverted membrane vesicles (IMVs) prepared from cells expressing either SecY–His_6–Myc *amber*–434 or *amber*–347 mutants in the presence of pBPA. They were UV-irradiated during incubation with purified SecA alone, in combination with ATP, or in combination with both ATP and proOmpA. Cross-linking with SecA at position 434 was markedly stimulated by the addition of both ATP and the preprotein (Fig. 5*A Upper*, lane 5). In contrast, pBPA at position 347 supported cross-linking with SecA equally well, irrespective of the presence or the absence of the translocation ligands (Fig. 5*A Lower*). These results reinforce the notion that interaction between SecA and C6 region of SecY is coupled with protein translocation reaction, but SecA interaction with the C5 loop is more constitutive or static.

N-Terminal Two-Thirds of SecA Is Involved in a Static Binding with SecY. The SecY–SecA cross-linked products show two electrophoretic mobilities. The product of the NaN_3-responsive cross-linking involving C6 migrates faster than the product of more static cross-link that is mediated by a C5 residue. We compared these two SecY positions to see whether they can be cross-linked with N-terminal ≈2/3 of SecA (Met-1–Lys-609; called N68) *in vitro*. The IMVs used above were mixed with N68 and UV-irradiated. A cross-linked product with N68 was observed significantly with the *amber–347* form of SecY–His_6–Myc (Fig. 5*B*, lane 3), but not with the *amber–434* form (Fig. 5*B*, lane 7) even

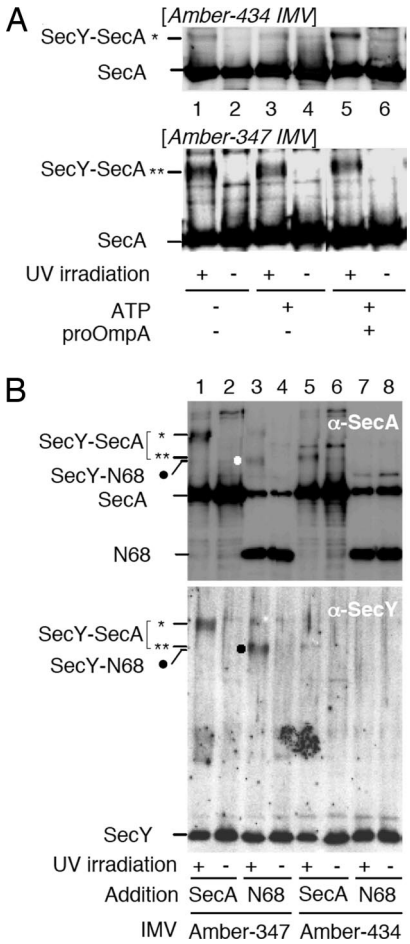

Fig. 5. *In vitro* photo-cross-linking at SecY positions 347 and 434. (*A*) Effects of concurrent translocation. IMVs (30 ng protein/μl) containing pBPA at indicated positions of SecY were mixed with SecA (5 ng/μl) and with ATP (5 mM) and proOmA (1 ng/μl) as indicated. Samples were incubated at 37°C for 20 min, UV-irradiated for 3 min, and analyzed by anti-SecA immunoblotting. (*B*) SecY C5 domain interacts with the N-terminal 2/3 of SecA. IMVs (30 ng protein/μl) containing pBPA at SecY positions 347 (lanes 1–4) or 434 (lanes 5–8) were mixed with 5 ng/μl of either SecA or its N68 fragment and incubated at 37°C for 5 min, followed by UV irradiation for 3 min as indicated. Membranes were analyzed by anti-SecA (*Upper*) and anti-SecY (*Lower*) immunoblottings. A new cross-linked product observed specifically with the combination of the *amber*-347 IMVs and N68 is indicated by the solid circle.

in the presence of ATP and proOmpA (data not shown). These results suggest that N68 that includes the ATPase domains of SecA is close to the C5 domain of SecY.

Discussion

Although Chin and Shultz (31) reported that their experimental system is effective in executing site-directed protein cross-linking *in vivo*, we have reported here its full-scale application to the residue-level *in vivo* analyses of protein–protein interactions in a biologically important molecular assembly. This approach is especially useful for dissecting the SecA–SecYEG interaction that changes during the course of protein translocation facilitation. We identified residues in cytoplasmic domains of SecY that are close enough to SecA to allow efficient cross-linking. Not all of the cytoplasmic domains contained such a residue. Thus, we failed to observe any SecA cross-linking at C1, at which cross-linking with SecY itself was observed (H.M., unpublished results) or at C3, at which cross-linking with SecG was observed. Involvement of these SecY regions in self-dimerization and SecG binding, respectively, is consistent with previous reports (19, 21).

The remaining cytoplasmic domains, C2, C4, C5, and C6, all contained residues cross-linkable with SecA. On the 3D structure model of SecY (2, 38), the side chains of Ser-111 (C2), Tyr-248 (C4), Ser-262 (C4), Lys-347 (C5), and Lys-434 (C6) all are located at or near the tips of the cytoplasmic protrusions (Fig. 6*A*). It is also notable that the majority of the residues that are in-close neighbors of SecA are in the C-terminal half of the pseudosymmetry units (Fig. 6*A*), as discussed by Van den Berg *et al.* (2), and are consistent with the implications from our genetic studies (6, 22, 24, 25). Ser-111 in the N-terminal half is in the proximity of both SecA and SecG (19), in line with the SecA-related functional roles assigned for SecG (39, 40). After completion of this work, van der Sluis *et al.* (41) identified two SecY regions as potential interaction sites with SecA, C5 identified by chemical cross-linking and the cytoplasmic end of TM4 identified by a peptide array binding assay. Whereas the former site agrees with our conclusion, the significance of the latter site should be validated by experiments using native materials. The *in vivo* approaches we used in this study will be useful for the analysis of SecY–SecA interactions involving transmembrane regions of SecY.

Treatment of cells with NaN_3 resulted in specific enhancement of SecA cross-linking with C6 residues, but not at other cytoplasmic domains of SecY. The NaN_3 response was lost by an additional mutation, either *secY205* or *prlA3* of *secY*. Previous studies suggest that the *secY205* mutation impairs the ability of SecY to support SecA functions, including its "insertion" (6), whereas the *prlA* mutations up-regulates the SecA-activating function of SecY (28, 42). Although the absolute levels of SecA cross-linking with these mutant forms of SecY should be compared by more quantitative experiments, we assume that these mutations abolish the NaN_3 effect on the cross-linking through different mechanisms. Our *in vitro* results lend direct support to our conclusion that C6 interacts preferentially with SecA that is actively delivering a preprotein into the translocon.

We propose that the C4–C5 region provides relatively constitutive binding sites for SecA. Our results using the C-terminally truncated SecA variant (N68) indicate that C5 is close to the N-terminal 2/3 of SecA. The ability of the N-terminal region of SecA to bind to SecYEG is consistent with a previous report (43). If the different SDS/PAGE mobilities of the cross-linked products reflect the positions of SecA responsible for the cross-linking, it seems possible that the slower migrating product is mediated by the N-terminal region of SecA, and the faster migrating product is formed at the C-terminal region of SecA (Fig. 6*B*). This possibility, along with more precise determination of the partner residues in SecA, remains left for further experimental analyses. At any rate, the present results reveal at least three different modes of SecA–SecY interactions: (*i*) a dynamic and function-related interaction involving C6 of SecY and giving the faster-migrating product, (*ii*) a static interaction involving C5 of SecY and the N-terminal part of SecA and giving the slower-migrating product, and (*iii*) a static interaction involving C4 and giving the faster-migrating product (Fig. 6*B*). It is possible that the interaction involving C2 is similar to the second interaction above.

We believe that the second interaction that occurs between the ATPase region of SecA and the C5 loop of SecY leads to the activation of SecA ATPase. A C5 residue Arg-357 was shown previously to be of particular importance for the SecY function in activating SecA (3, 24). On the other hand, the first interaction involving C6 is related to the event, in which SecA actively drives translocation. These interpretations are consistent with our genetic observation that ATPase activation and preprotein translocation are separable (58). The fact that a number of the C6 residues can be cross-linked to SecA might imply that SecA

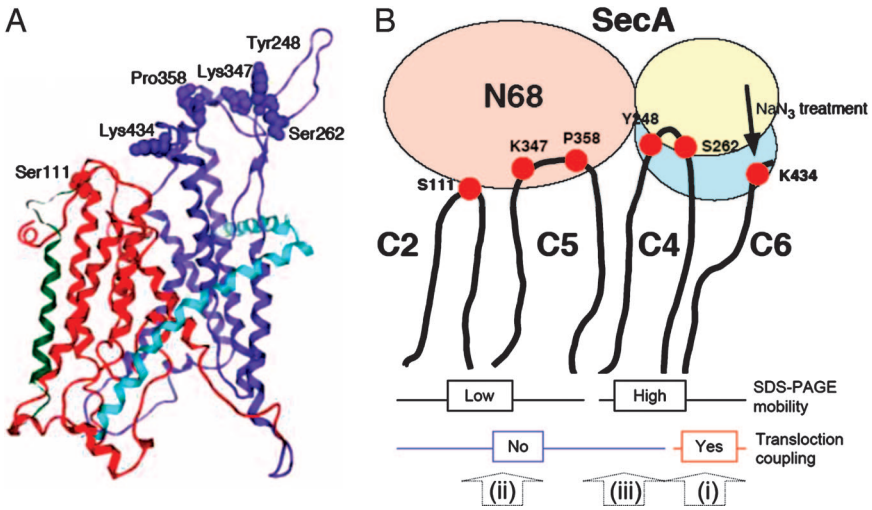

Fig. 6. Different modes of SecA–SecY binding suggested by the cross-linking results. (*A*) Location of the SecY residues identified as SecA neighbors in the 3D structure model. *E. coli* SecY was modeled by using the MOE software (38) on the basis of the structure of *Methanococcus jammaschii* SecYEβ (2). The pseudosymmetrical halves of SecY (ribbon representation) are shown in red for TM1–TM5 and blue for TM6–TM10. SecE and Secβ are shown for reference purpose in pale blue and green, respectively, as unaltered *M. jammaschii* subunits. Side chains of the indicated residues, identified as SecA neighbors, are space-filled. (*B*) A schematic representation of different modes of SecA–SecY binding suggested by the present results. The different electrophoretic mobilities of the cross-linked products are assumed to result from the cross-linked positions on SecA, within the N-terminal 2/3 (N68) region for the lower mobility and within the C-terminal 1/3 domain for the higher mobility. The cross-linking via the C6 residues is enhanced by ongoing translocation reaction. The present study revealed three different modes (*i*, *ii*, and *iii*) of interaction between SecA and SecY.

is actually moving along the C6 region of SecY. This speculative notion is consistent with the involvement of the C6 region in the ATP- and preprotein-dependent SecA insertion event (6, 25). A recent report (44) also suggests that SecA undergoes extensive conformational changes upon binding to the translocon. The NaN_3 stimulation of type *i* cross-linking agrees excellently with the reported ability of this reagent to stabilize the inserted state of SecA (34). While our present studies provide a framework for our further understanding of SecA–SecY interactions, fundamental issues, the oligomeric state of the working state of SecA (45–48), and that of the active form of SecYEG (12, 14, 15, 17, 18), remain to be addressed by more direct structural analysis.

Materials and Methods

Chemicals and Media. pBPA was purchased from Bachem (Bubendorf, Switzerland). For *in vivo* cross-linking experiments cells were grown on minimal M9 medium (49) supplemented with glucose (0.4%), pBPA (1 mM), $CaCl_2$ (5 mM), ampicillin (50 μg/ml), and either chloramphenicol (20 μg/ml; for pHM649-harboring cells), kanamycin (25 μg/ml; for pHM640-harboring cells), or tetracycline (50 μg/ml; for pDUEL-Tyr-harboring cells). L medium contained 10 g of bactotryptone, 5 g of yeast extracts, and 5 g of NaCl per liter.

Bacterial Strains and Plasmids. *E. coli* K-12 strain MC4100 [F^- *araD139* Δ(*argF-lac*)*U169 rpsL150 relA1 flbB5301 deoC1 ptsF25 rbsR* (49)] or its *ompT*::*Kan*^{r} derivative, AD202 (50) was used for *in vivo* cross-linking experiments. JM109 (51) was used for gene manipulation.

pDUEL-Tyr is the original Tet^R plasmid encoding the mutant MjtRNA and the mutant MjRS (52), which allow amber codon suppression by incorporating pBPA. pHM640 and pHM649 were its derivatives having Km^R marker (from pUC4K obtained from Takara, Tokyo, Japan) or Cm^R marker [from pHP45Ω-Cm (53)], respectively, inserted into the EagI site within the Tet^R marker gene. Amber mutants of SecY–His_6–Myc on pNA3 (54) were constructed by replacing specified *secY* codons with TAG, using the QuikChange procedures (Strategene, La Jolla, CA), followed by confirmation of the nucleotide sequences.

***In Vivo* Photo-Cross-Linking.** Two plasmids, one (pDUEL-Tyr, pHM640, or pHM649) endowing the host cell with the ability to incorporate pBPA in response to an *amber* codon and another expressing an *amber* mutant form of SecY–His_6–Myc, were introduced into either strain MC4100 (for pHM640) or strain AD202 (for pDUEL-Tyr or pHM649). The transformed cells were grown at 37°C on M9-glucose medium supplemented with pBPA to a midlog phase, at which a portion (1 ml) of the culture was transferred to a Petri dish and irradiated with UV (365 nm) for 3 min by using a B-100AP (Ultraviolet Products, Upland, CA) UV lamp at a distance of 4 cm. Irradiated cells were collected by centrifugation, washed with 10 mM Tris·HCl (pH 8.1), and suspended in 400 μl of Tris·HCl (pH 7.5), 1 mM EDTA, and 0.1 mM Pefabloc (Merck, Whitehouse Station, NJ). Cells were disrupted by freezing-thawing and sonication [Heat Systems (Farmingdale, NY) sonicator] with cooling on ice. After removal of debris materials by centrifugation [13,000 rpm for 10 min at 4°C with a TOMY SEIKO (Tokyo, Japan) MRX-150 centrifuge], membranes were precipitated by ultracentrifugation [45,000 rpm for 30 min at 4°C with a Hitachi (Tokyo, Japan) S45A rotor] and solubilized with 1% SDS at 37°C for 60 min. Proteins were separated by SDS/PAGE (55) and detected by immunoblotting (56) using antiserum against SecY, SecA, SecG, or Myc. Protein concentrations of SecA and IMVs preparations were determined by A_{280} (molar adsorption coefficient of SecA assumed to be 1.0×10^5) and the Bradford method, respectively.

Other Materials. SecA and its N68 fragment were purified as described (57). IMVs were prepared as described (24).

We thank Peter G. Schultz of The Scripps Research Institute (La Jolla, CA) for the kind gift of pDUEL-Tyr and the experimental protocols for *in vivo* photo-cross-linking; Joachim Frey (University of Bern, Bern, Switzerland) for pHP45Ω-Cm; Naomi Shimokawa (Kyoto University) for initial *in vitro* SecY–SecA cross-linking trials and suggestions on the target SecY positions; Yoshinori Akiyama and Kenji Inaba for helpful discussion; and Kiyoko Mochizuki, Michiyo Sano, and Takuya Adachi for technical support. This work was supported by grants from the Japan Society for the Promotion of Science; the Ministry of Education, Culture, Sports, Science, and Technology, Japan; Core Research for Evolutional

Science and Technology; the Japan Science and Technology Agency; and the National Project on Protein Structural and Functional Analyses of the Ministry of Education, Culture, Sports, Science, and Technology, Japan.

1. Osborne AR, Rapoport TA, van den Berg B (2005) *Annu Rev Cell Dev Biol* 21:529–550.
2. Van den Berg B, Clemons WM, Jr, Collinson I, Modis Y, Hartmann E, Harrison SC, Rapoport TA (2004) *Nature* 427:36–44.
3. Mori H, Ito K (2001) *Trends Microbiol* 9:494–500.
4. Veenendaal AK, van der Does C, Driessen AJ (2004) *Biochim Biophys Acta* 1694:81–95.
5. Vrontou E, Economou A (2004) *Biochim Biophys Acta* 1694:67–80.
6. Matsumoto G, Yoshihisa T, Ito K (1997) *EMBO J* 16:6384–6393.
7. Economou A, Wickner W (1994) *Cell* 78:835–843.
8. Akiyama Y, Ito K (1987) *EMBO J* 6:3465–3470.
9. Cannon KS, Or E, Clemons WM, Jr, Shibata Y, Rapoport TA (2005) *J Cell Biol* 169:219–225.
10. Manting EH, van Der Doesqq C, Remigy H, Engel A, Driessen AJ (2000) *EMBO J* 19:852–861.
11. Breyton C, Haase W, Rapoport TA, Kuhlbrandt W, Collinson I (2002) *Nature* 418:662–665.
12. Mori H, Tsukazaki T, Masui R, Kuramitsu S, Yokoyama S, Johnson AE, Kimura Y, Akiyama Y, Ito K (2003) *J Biol Chem* 278:14257–14264.
13. Duong F (2003) *EMBO J* 22:4375–4384.
14. Mitra K, Schaffitzel C, Shaikh T, Tama F, Jenni S, Brooks CL, 3rd, Ban N, Frank J (2005) *Nature* 438:318–324.
15. Douville K, Price A, Eichler J, Economou A, Wickner W (1995) *J Biol Chem* 270:20106–20111.
16. Lill R, Cunningham K, Brundage LA, Ito K, Oliver D, Wickner W (1989) *EMBO J* 8:961–966.
17. Manting EH, van der Does C, Driessen AJ (1997) *J Bacteriol* 179:5699–5704.
18. Snyders S, Ramamurthy V, Oliver D (1997) *J Biol Chem* 272:11302–11306.
19. Satoh Y, Matsumoto G, Mori H, Ito K (2003) *Biochemistry* 42:7434–7441.
20. Satoh Y, Mori H, Ito K (2003) *Biochemistry* 42:7442–7447.
21. van der Sluis EO, Nouwen N, Driessen AJ (2002) *FEBS Lett* 527:159–165.
22. Taura T, Yoshihisa T, Ito K (1997) *Biochimie* 79:517–521.
23. Mori H, Ito K (2001) *Proc Natl Acad Sci USA* 98:5128–5133.
24. Mori H, Ito K (2003) *J Bacteriol* 185:405–412.
25. Chiba K, Mori H, Ito K (2002) *J Bacteriol* 184:2243–2250.
26. Baba T, Jacq A, Brickman E, Beckwith J, Taura T, Ueguchi C, Akiyama Y, Ito K (1990) *J Bacteriol* 172:7005–7010.
27. Matsumoto G, Nakatogawa H, Mori H, Ito K (2000) *Genes Cells* 5:991–999.
28. van der Wolk JP, Fekkes P, Boorsma A, Huie JL, Silhavy TJ, Driessen AJ (1998) *EMBO J* 17:3631–3639.
29. Mori H, Shimizu Y, Ito K (2002) *J Biol Chem* 277:48550–48557.
30. Chin JW, Martin AB, King DS, Wang L, Schultz PG (2002) *Proc Natl Acad Sci USA* 99:11020–11024.
31. Chin JW, Schultz PG (2002) *ChemBioChem* 3:1135–1137.
32. Dorman G, Prestwich GD (1994) *Biochemistry* 33:5661–5673.
33. Oliver DB, Cabelli RJ, Dolan KM, Jarosik GP (1990) *Proc Natl Acad Sci USA* 87:8227–8231.
34. Eichler J, Rinard K, Wickner W (1998) *J Biol Chem* 273:21675–21681.
35. Osborne RS, Silhavy TJ (1993) *EMBO J* 12:3391–3398.
36. Taura T, Akiyama Y, Ito K (1994) *Mol Gen Genet* 243:261–269.
37. Matsumoto G, Homma T, Mori H, Ito K (2000) *J Bacteriol* 182:3377–3382.
38. Mori H, Shimokawa N, Satoh Y, Ito K (2004) *J Bacteriol* 186:3960–3969.
39. Matsumoto G, Mori H, Ito K (1998) *Proc Natl Acad Sci USA* 95:13567–13572.
40. Suzuki H, Nishiyama K, Tokuda H (1998) *Mol Microbiol* 29:331–341.
41. van der Sluis EO, Nouwen N, Koch J, de Keyzer J, van der Does C, Tampe R, Driessen AJ (2006) *J Mol Biol* 361:839–849.
42. Duong F, Wickner W (1999) *EMBO J* 18:3263–3270.
43. Dapic V, Oliver D (2000) *J Biol Chem* 275:25000–25007.
44. Natale P, den Blaauwen T, van der Does C, Driessen AJ (2005) *Biochemistry* 44:6424–6432.
45. Or E, Boyd D, Gon S, Beckwith J, Rapoport T (2005) *J Biol Chem* 280:9097–9105.
46. de Keyzer J, van der Sluis EO, Spelbrink RE, Nijstad N, de Kruijff B, Nouwen N, van der Does C, Driessen AJ (2005) *J Biol Chem* 280:35255–35260.
47. Jilaveanu LB, Oliver D (2006) *J Bacteriol* 188:335–338.
48. Jilaveanu LB, Zito CR, Oliver D (2005) *Proc Natl Acad Sci USA* 102:7511–7516.
49. Silhavy TJ, Berman ML, Enquist LW (1984) *Experiments with Gene Fusions* (Cold Spring Harbor Lab Press, Cold Spring Harbor, NY).
50. Akiyama Y, Ito K (1990) *Biochem Biophys Res Commun* 167:711–715.
51. Yanisch-Perron C, Vieira J, Messing J (1985) *Gene* 33:103–119.
52. Farrell IS, Toroney R, Hazen JL, Mehl RA, Chin JW (2005) *Nat Methods* 2:377–384.
53. Prentki P, Krisch HM (1984) *Gene* 29:303–313.
54. Mori H, Akiyama Y, Ito K (2003) *J Bacteriol* 185:948–956.
55. Ito K, Cerretti DP, Nashimoto H, Nomura M (1984) *EMBO J* 3:2319–2324.
56. Shimoike T, Akiyama Y, Baba T, Taura T, Ito K (1992) *Mol Microbiol* 6:1205–1210.
57. Nakatogawa H, Mori H, Ito K (2000) *J Biol Chem* 275:33209–33212.
58. Mori H, Ito K (2006) *J Biol Chem*, in press.